Chapter 3
Naturally occurring uranium in the Boom Clay

Contents

3.1 Introduction

The knowledge of the uranium migration in the Boom Clay is mainly acquired from laboratory experiments which are limited in time and space. The extrapolation of the uranium behaviour based on these small-scale and short-term experiments to large-scale and long-term behaviour remains difficult. Complementary evidences on the long-term geochemical processes controlling the uranium migration may be derived from the study of uranium naturally present in the Boom Clay. Indeed, the study of naturally occurring uranium provides information on the long-term behaviour of uranium in real conditions and over geological time-periods.

In this chapter, we will first present the state-of-the art on the concentration and mobility of naturally occurring uranium in the Boom Clay. Most of the data come from the publication by Yoshida *et al.* (1991) and from the natural analogue study on the Boom Clay started in 1996 (De Craen *et al.*, 2000). Second, we have determined the uranium content in several rock-forming or accessory Boom Clay minerals to better characterise naturally occurring uranium.

3.2 Concentration of natural uranium in Boom Clay pore water

Yoshida *et al.* (1991) reported a mean value for the uranium concentration in Boom Clay pore water of about 2×10^{-9} mol·l^{-1} (0.5 ppb). Uranium concentrations varying between 1.4×10^{-10} to 4.4×10^{-8} mol·l^{-1} (0.03 - 10.5 ppb) are reported by Dierckx *et al.* (2000) and De Craen *et al.* (in preparation) in water samples collected from piezometers in the underground research laboratory. Generally, the uranium concentration is less than 4.2×10^{-9} mol·l^{-1} (1 ppb). All measurements fall in the range of 10^{-10} to 10^{-8} mol·l^{-1} and these values are considered as the concentration of mobile natural uranium in the Boom Clay.

The uranium concentrations in the aquifers above and below the Boom Clay are also in the range of 10^{-10} to 10^{-9} mol·l^{-1} (Marivoet *et al.*, 2000). The similar uranium concentrations measured in Boom Clay pore water and in surrounding aquifers indicate a very homogeneous distribution of mobile uranium. There should be no diffusion from the Boom Formation to the aquifers. The alike concentrations also suggest that the dissolved uranium concentration might be solubility controlled by an uranium-bearing phase existing in the system (Dierckx *et al.*, 2000).

Recently, uranium series disequilibrium studies have been performed on pore water derived from the MORPHEUS piezometer (De Craen *et al.*, in preparation). The $^{234}U/^{238}U$ activity ratios are indicative of isotopic disequilibrium with $^{234}U/^{238}U$ activity ratios between 1 and 5. An excess of ^{234}U relative to ^{238}U is a common observation in natural waters (Fleisher, 1988). This isotopic disequilibrium results from α-recoil, either as the direct ejection of the recoil ^{234}U atom into the pore water, or indirectly by the preferential leaching of the products of alpha decay, *i.e.* ^{234}U.

3.3 Concentration profile of natural uranium in the Boom Clay

The overall uranium content in the Boom Clay typically varies between 3 and 6 ppm with a mean value of 4 ppm (Yoshida *et al.*, 1991; De Craen *et al.*, 2000). Normalized to the North American Shale Composite (Gromet *et al.*, 1984), the Boom Clay shows an enrichment factor in uranium of 1.5 by considering an average content of 4 ppm.

The general shape of the uranium profile reflects decreasing uranium concentration towards the upper and lower stratigraphic levels of the Boom Clay (De Craen *et al.*, 2000). Superimposed on the general shape, four horizons with a higher uranium concentration are recognised. The most important level with higher uranium concentration, containing up to 13 ppm uranium, occurs at the base of the Putte Member. The variations in uranium content are considered to be primary in origin since they are mainly related to lithological variations in the deposit such as changes in the clay, uranium-bearing minerals and organic matter content (De Craen *et al.*, 2000). The decreasing uranium concentration at the upper and lower stratigraphic levels can be explained by lithological variations as well since the Boom Clay is more silty and contains less organic matter at these levels. Another likely explanation is the influence of the over- and underlying aquifers of which the ground waters might have redistributed or removed some of original uranium.

3.4 Mobility of natural uranium in the Boom Clay

Yoshida *et al.* (1991) determined an "*in situ*" ratio of uranium in the clay to uranium in the pore water of 2000. According to the authors, this high distribution coefficient and the unity value of the activity ratios of uranium isotopes and daughters indicate that uranium is essentially immobile in the Boom Clay.

More recently, new radiochemical studies have been performed to study the mobility of natural uranium in the Boom Clay on a geological time scale (De Craen *et al.*, 2000). The radiochemical data on bulk Boom Clay show that in the entire Boom Clay profile, the $^{234}U/^{238}U$ and $^{230}Th/^{234}U$ activity ratios are close to unity within the 2σ uncertainty, although there might be some evidence for ^{234}U excess in some samples. This means that no significant mobility of the isotopes of the uranium decay series has been detected at least for the last million years. The ^{234}U excess in some samples is explained by equilibrium with the pore water which is characterized by ^{234}U excess as a result of α-recoil (Fleisher, 1988). From the U-Th series disequilibrium studies, it is clear that the higher uranium concentration at the base of the Putte Member is not associated with radioactive disequilibrium, suggesting that the higher uranium concentration is not the result of secondary processes, at least not within the last one million years. One exception is the 'double band", the most silty layer of the Boom Clay. This zone of higher permeability is consequently a zone of potential higher mobility for uranium species as indicated by the $^{230}Th/^{234}U$ activity ratio significantly larger than 1 (~1.35).

3.5 Uranium content in Boom Clay minerals

3.5.1 Literature review

According to Yoshida *et al.* (1991), the examination of the uranium distribution by fission track prints indicates three principal types of location. Uranium is generally dispersed throughout the sediment, presumably associated with surfaces of clay particles, amorphous oxy-hydroxides or finely dispersed organic material. Much higher local concentrations (several hundreds of ppm) are related to detrital mineral grains, principally zircon but including other species such as monazite and apatite. A significant amount of uranium is also found in intimate association with plant debris where levels of several hundred ppm uranium are attained. The authors did not observe uranium concentration in association with pyrite.

Laenen (1997) measured the uranium content in the clayey fraction (< 2 μm), in glauconite and fossil biogenic apatite. The average uranium concentration measured in the clayey fraction of 79 Boom Clay samples is 4 ppm. With uranium content of about 5 ppm, glauconites are moderately enriched compared to the surrounding sediment and the clayey fraction. In biogenic apatite, the uranium concentration varies generally between 10 and 30 ppm. However, uranium content up to 78 ppm was measured at the base of the Putte Member (Laenen *et al.*, 1997). Laenen (1997) also reported that uranium is not directly associated with calcite.

Statistical analyses performed in the frame of the natural analogue study on the Boom Clay point out that uranium is mainly associated with organic matter, apatite, calcite and siderite (De Craen *et al.*, 2000).

In conclusion, the association of uranium and organic matter is clearly established by Yoshida *et al.* (1991) and De Craen *et al.* (2000). This association probably results from the uranium reduction and its subsequent immobilisation (see also 2.4.2.2). The higher uranium concentration in biogenic apatite relative to the bulk sediment measured by Laenen (1997) is confirmed by statistical analyses which show a good correlation between uranium and P_2O_5 (De Craen *et al.*, 2000). However, the uranium association with carbonates postulated from statistical analyses by De Craen *et al.* (2000) is in contradiction with the finding of Laenen (1997) who noted no uranium association with calcite. These observations would indicate that the uranium association with carbonates is mainly due to siderite. Therefore, the role of siderite needs to be investigated more in detail. De Craen *et al.* (2000) defined three groups of minerals to explain the trace elements distribution in the Boom Clay, and namely a group containing apatite, calcite, pyrite, and organic matter. This group concentrates lutetium and uranium. However, Yoshida *et al.* (1991) did not observe uranium concentration in association with pyrite. Again, more information is needed to verify the role of pyrite in the uranium distribution in the Boom Clay.

The objective of this study is to separate and characterize different mineralogical phases or fractions from Boom Clay bulk samples and to measure the concentration of natural uranium to verify some questionable uranium association with minerals.

3.5.2 Samples preparation

3.5.2.1 Bulk samples

Two bulk Boom Clay samples were taken in the Putte Member, either in open pit or in underground research laboratory. The first sample (**S-50**) was taken on May 23rd 2000 at the "Swenden" quarry (Rumst, Belgium) in the septaria horizon S50 (Figure 3.1). After sampling, the clay was preserved in a dark cold room at 6°C and allowed to dry. The second bulk Boom Clay sample (**CTP-00**) was taken during the excavation of the connecting gallery in the underground research laboratory on February 20th and 27th 2002 (Figure 3.1). To prevent possible oxidation by oxygen, the sample was immediately packed under vacuum in aluminium-coated poly-ethylene sheets and stored in a dark cold room at 6°C.

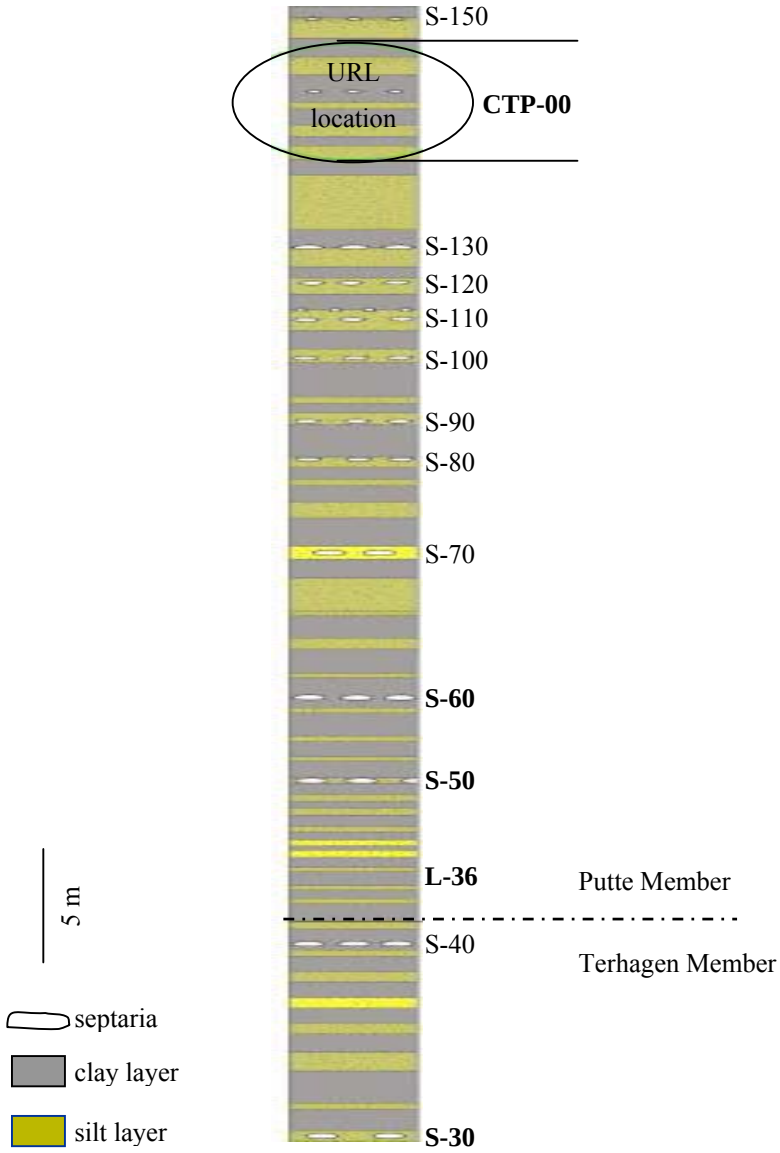

Figure 3.1. Lithostratigraphic profile showing the sample location; URL: underground research laboratory (profile from Nirond 2003-02).

3.5.2.2 Magnetic and non-magnetic fractions

The magnetic and non-magnetic fractions were separated from the bulk Boom Clay sample **CTP-00**. The separation was carried out at the Centre Terre et Pierre (Tournai, Belgium). The sample was first disintegrated in water by hand and further by mechanic agitation. After sieving at 1.25 mm, the slurry was treated with a centrifugal gravimetric separator (Knelson concentrators, KC MD3). The mineral slurry is flowed in a ribbed cone rotating at a centrifugal force of about 60g. During the process, the heavy fraction becomes trapped within the inter-ribs space. Water is injected through series of perforations in the cone's wall to keep the material totally fluidized and to allow heavier particles to continuously displace lighter particles (Figure 3.2). Two water counter-pressures were used for our treatment: 20 and 10 kPa, respectively.

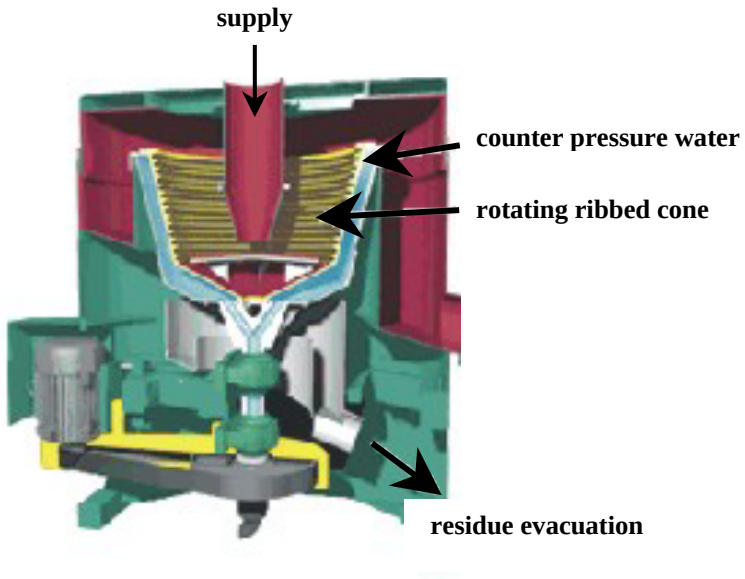

Figure 3.2. Schematic representation of the centrifugal gravimetric separator (Knelson concentrator).

The heavy fractions recovered from the ribbed cone were afterwards handled with a high gradient wet magnetic separator (Carpco). This magnetic separator allows to separate diamagnetic minerals from paramagnetic minerals. The separation is performed by applying an intensive magnetic field created by two coils on iron balls (∅ = 19 mm) on which the fluidised material is versed (Figure 3.3). The paramagnetic minerals are retained by the iron balls while the diamagnetic minerals flow with the water flux and are then collected. The paramagnetic minerals are recovered by rinsing the iron balls once the magnetic field is cut. Two current intensities were applied on the coils: 2 and 4 amperes. Magnetic and non-magnetic fractions were further purified by using a dry magnetic separator (Frantz) operating at a current of 1.5 amperes and lateral and longitudinal dips of 10 and 25°, respectively.

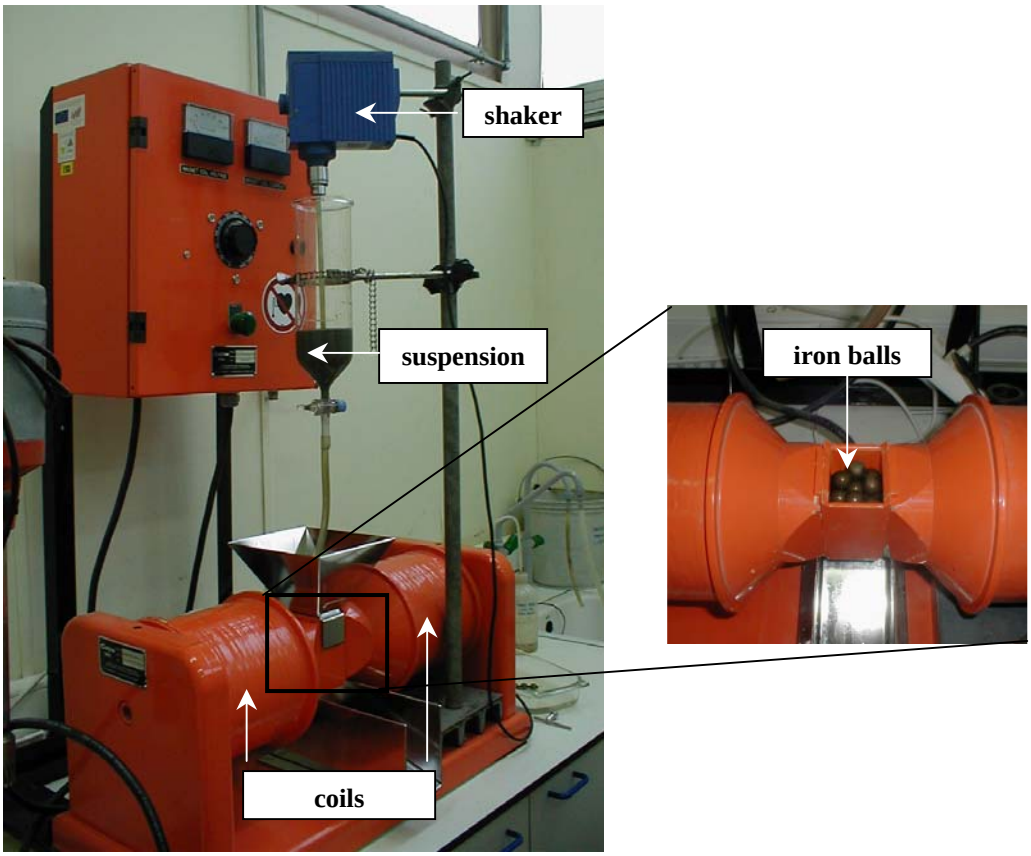

Figure 3.3. General and detailed pictures of the high gradient wet magnetic separator (Carpco).

3.5.2.3 Clayey fraction

The residue coming from the centrifugal gravimetric separator was hydrocycloned to remove the particles larger than 15 μm. The hydrocyclone was supplied with the residue of the Knelson concentrator at a pressure of 2.2 bars. Due to the centrifuge force, the coarse grains are thrown to the hydrocyclone walls and go down towards the cone hole where they are evacuated (Figure 3.4). This fraction forms the underflow and was used for pyrite separation by flotation (3.5.2.4). On the other hand, the fine particles (< 15 μm) swept along with the water flux go up following an ascending helical movement, go through to the diaphragm and are recovered. This fraction constitutes the overflow (Figure 3.4). The clayey fraction (< 2 μm) was separated from the overflow by sedimentation according to the Stokes law. The 2 μm-suspensions were sampled and the clay particles were concentrated either by centrifugation or by flocculation with $SrCl_2.6H_2O$.

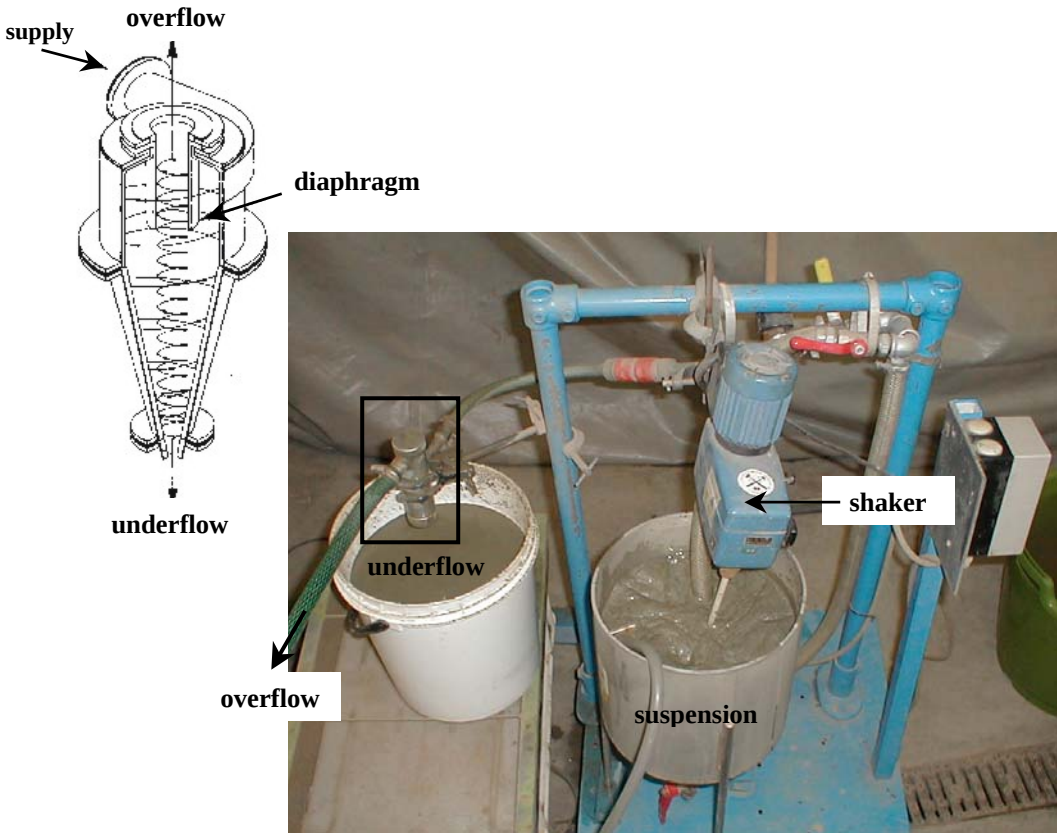

Figure 3.4. Picture and detailed schematic representation of the hydrocyclone.

3.5.2.4 Pyrite

Special precautions were taken to avoid pyrite oxidation: (i) all pyrite samples were extracted from bulk Boom Clay samples preserved under vacuum in aluminium-coated poly-ethylene sheets and stored in a dark cold room at 6°C, (ii) pyrite was stored under water column before drying, (iii) pyrite was dried with acetone to avoid prolonged contact with water under atmospheric conditions, and (iv) pyrite was stored in a desiccator or in a glove box.

Three samples of pyrite were obtained from the bulk Boom Clay sample CTP-00 by three different separation methods. Pyrite occurring as concretionary bodies was separated by wet sieving at 1.25 mm (**CTP-+1.25 mm**). The sample **CTP-heavy** resulted from the concentration of heavy minerals of a non-magnetic fraction in heavy liquid (bromoform). Framboidal pyrite (< 15 μm) was obtained by flotation of the underflow concentrated by the hydrocyclone (**CTP-flotation**).

One pyrite sample came from a bulk Boom Clay sample taken at the "Swenden" quarry (Rumst, Belgium) in the layer **L-36** (Figure 3.1). Pyrite was separated by disintegrating the bulk sample in water and sieving at 1 mm. Pyrite was collected by hand picking and washed ultrasonically 10 times for periods never exceeding 2 minutes (Sonifier 250, Branson).

3.5.2.5 Carbonates

Bivalve shells were separated from the bulk Boom Clay sample taken at the "Swenden" quarry (Rumst, Belgium) in the septaria horizon S50 (Figure 3.1). Bivalve shells were concentrated by disintegrating the bulk sample in water and by sieving at 1 mm. Shell fragments were collected from the residue by hand picking. These fragments were washed ultrasonically 5 times for 20 seconds (Sonifier 250, Branson).

Carbonate concretions (septaria) were sampled on November 6th 2002 at the "Argex" quarry (Kruibeke, Belgium) from three different levels: S30, S50 and S60 (Figure 3.1).

3.5.3 Results

All minerals or mineralogical fractions were characterised by x-ray diffraction (XRD) at the Cellule Interdépartementale d'Analyse, faculty of Sciences of the University of Louvain-la-Neuve (Belgium). A Siemens D500 diffractometer working with the mean Cu Kα line (λ=1.5418 Å) was used for standard powder diffraction. The scan speed was 0.5°2θ per 60 seconds. Scans of the various diffraction peaks were recorded in the 4°-90°2θ range, except for the clayey fraction for which the range was 2°-30°2θ. The results were interpreted with SOCABIM DiffracPlus version 5.1 software. The mineral quantification was performed with the quantitative powder XRD phase analysis software Siroquant version 2.5 (Sietronics, Australia).

The scanning electron microscopy (SEM) analyses were carried out at SCK•CEN in the microstructure research group with a fully shielded Jeol 6310 Scanning Electron Microscope.

The uranium content was measured by Inductively Coupled Plasma-Mass Spectrometry (Sciex 5000, Perkin-Elmer ICP-MS). The 95% confidence interval 2σ on uranium concentration was about 20%. The minerals were dissolved by alkaline fusion: 0.25 g of the grounded sample were mixed with 1.25 g of lithium borate (Spectroflux type 100B) and heated at 1000°C for 40 minutes. The hot melt is poured into 150 ml of 0.8 M HNO_3, stirred for 1 hour or longer and diluted to 250 ml in a volumetric flask. This solution was further diluted 20 times prior to analysis. The analyses were performed at the Laboratory of Analyses and Applied Radiochemistry, Nuclear Chemistry and Services (SCK•CEN, Belgium).

3.5.3.1 Bulk samples

The uranium content in the bulk sample CTP-00 is 3.5 ppm. Such uranium concentration is similar to the generally reported uranium content in the Boom Clay, *i.e.* 4 ppm (Yoshida *et al.*, 1991). The bulk sample S-50 is enriched in uranium relative to the sample CTP 00 since it contains 7 ppm uranium. X-ray diffraction analyses indicate that both samples contain clay minerals, feldspars and pyrite. The sample S-50 also contains about 11 wt. % calcite and 3 wt. % gypsum. Gypsum results from the pyrite oxidation occurring in the open pits. Therefore, the higher uranium content in sample S-50 is ascribed to the presence of calcite. This observation supports the results of the statistical analyses which have shown an association between uranium and calcite (De Craen *et al.*, 2000).

3.5.3.2 Magnetic fractions

The magnetic fractions are enriched in uranium, with uranium content varying between 9 and 12 ppm. These fractions are mainly composed of quartz, glauconite and carbonates (Table 3.1).

Table 3.1. Uranium content and mineralogical composition of the magnetic fractions.

Magnetic fraction	Uranium content	Mineralogical composition (wt.%)					
	ppm	quartz	glauconite	siderite	dolomite	pyrite	feldspar
1	11.9	43	38	—	4	3	12
2	10.2	25	45	25	2	2	1
3	9.5	59	25	—	2	13	1
4	9.2	22	36	32	9	1	—

Glauconite is not detected as such by XRD analyses. The presence of glauconite is postulated on the basis of the peaks occurrence at 14 and 10 Å in the diffraction pattern of all magnetic fractions. Indeed, the XRD analyses on glauconite show that they consist of a group of clays with a mineralogical composition ranging from smectite to illite (Laenen, 1997). The content of glauconite reported in the Table 3.1 is consequently determined by considering the sum of the weight percentages of clay minerals identified by XRD as chlorite, illite or muscovite. Although light to dark green grains were recognized by eye and binocular in the magnetic fractions, the presence of glauconite was independently verified by SEM analyses (Figure 3.5). Rounded grains with a size ranging between about 75 and 150 μm whose the qualitative chemical composition analysed by energy dispersive x-ray (EDX) is O, Mg, Al, Si, K, Ca, and Fe are easily identified as glauconite.

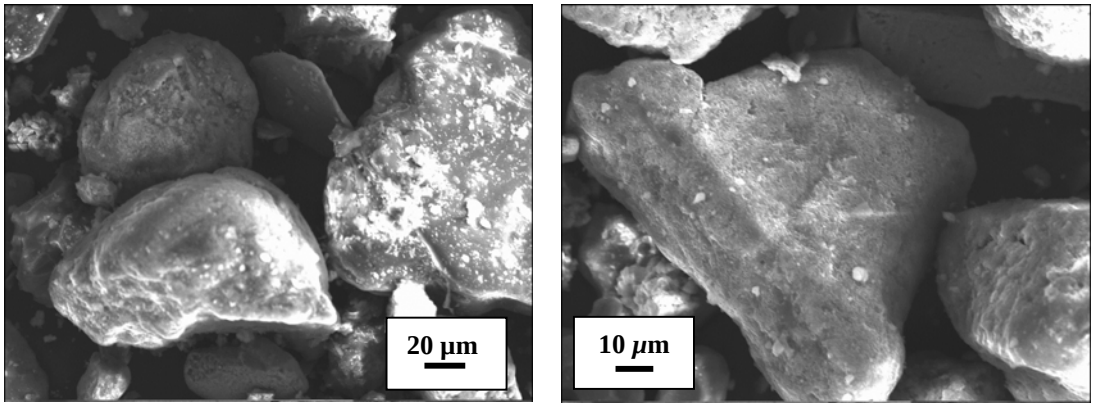

Figure 3.5. Micrographic images of glauconite in the magnetic-fractions.

According to Laenen (1997), diffraction peaks of glauconite also occur at 4.28 and 3.34 Å and originate from quartz relicts, indicating that quartz may have been subjected to glauconitisation. The glauconitisation of quartz would explain its relatively high content in the magnetic fractions (Table 3.1). Quartz is also often found as inclusions in glauconite (Vandenberghe, 1978).

The carbonates of the magnetic fractions have a composition varying from dolomite ($Ca,Mg(CO_3)_2$) to siderite ($FeCO_3$), and including ankerite ($Ca,Fe(CO_3)_2$). This indicates that the iron content is variable in the carbonates of the Boom Clay. Since dolomite is a non-magnetic mineral, it probably contains some iron to be concentrated in the magnetic fractions. Calcite is not present in the magnetic fractions. Scanning electron microscope analyses show that the carbonates occur as small rhombohedral crystals, sometimes with curved faces, with a size between 2 and 5 μm (Figure 3.6). More rarely, the crystals have a prismatic or scalenohedral habit. These small crystals do not occur dispersed but assembled into rounded grains with a size ranging from about 30 to 250 μm (Figure 3.6). In these assemblages, carbonate crystals occur together with clay particles (Figure 3.6). The chemical elements identified by EDX analyses of the grains composed of the carbonates-clay minerals association are mainly C, O, Ca, Fe and Mg but the peak of Si is also identified. The chemical composition corresponds to the composition of iron-rich dolomite, ankerite and siderite. Silicon results from the presence of clay minerals.

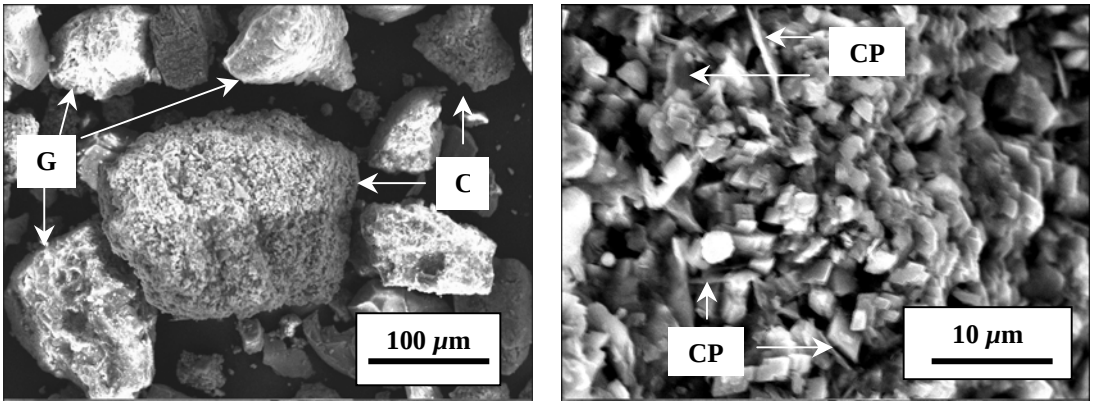

Figure 3.6. Micrographic pictures of the carbonates-clay minerals assemblages; G: glauconite, C: carbonates; CP: clay particles.

The enrichment of uranium in the magnetic-fractions emphasises the role of authigenic iron-bearing minerals such as glauconite and siderite in the uranium distribution in the Boom Clay. However, the contribution to the uranium content of paramagnetic heavy minerals occurring in concentrations below the XRD detection limit such as xenotime and monazite is probably non-negligible.

3.5.3.3 Non-magnetic fractions

The non-magnetic fractions are relatively poor in uranium with uranium content lower than 3 ppm. The mineralogical assemblage detected by XRD in these fractions is mainly composed of quartz, feldspar and pyrite (Table 3.2).

The lower uranium concentration in the non-magnetic fractions relative to the mean uranium content in the Boom Clay indicates that quartz, feldspar and pyrite do not concentrate uranium. We assume that the uranium content results from the contribution of non-magnetic minerals present in traces such as zircon and titanium oxides, for example.

Table 3.2. Uranium content and mineralogical composition of the non-magnetic fractions; n.d.: non determined.

Non-magnetic fraction	Uranium content	Mineralogical composition (wt.%)		
	ppm	quartz	feldspar	pyrite
1	2.9	n.d.	n.d.	n.d.
2	1.8	84	9	7
3	1.8	~ 100	—	—

3.5.3.4 Clayey fraction

The clayey fraction was analysed on oriented mounts under ambient room conditions (N), after heating at 500°C (F) and after exposure overnight to an ethylene glycol atmosphere (EG). The N, F and EG diffractograms of the clayey fraction are shown in Figure 3.7.

The N and EG diffraction patterns show sharp 7 Å (001) and (002)-reflections occurring at 12.3 and 24.9°2θ, respectively. These peaks do not change on EG treatment and are removed by heating at 500°C. This behaviour indicates the presence of kaolinite. The presence of small amount of chlorite is apparent from 14 Å (002) and (004)-reflections at 12.3 and 24.9°2θ on the diffractogram of the heated sample (F). Illite is also present as indicated by the occurrence in all XRD patterns of 10 Å (001), (002) and (003)-reflections at 8.8, 17.8 and 26.8°2θ, respectively. The presence of smectite can be deduced from the peak at 13.8 Å on the N diffraction pattern that expands to 16.7 Å on EG treatment and collapses to 10 Å on heating at 500°C. The presence of illite-smectite mixed layer is concluded from the occurrence of a broad peak between 10 and about 14 Å on the N pattern. Similar to smectite, the mixed-layer minerals expand towards 17 Å in the EG-saturated sample and collapse to 10 Å in the sample heated at 500°C. In accordance with the generally accepted clay mineralogy of the Boom Clay, the clayey fraction is composed of kaolinite, illite, smectite, illite-smectite mixed layer and minor amounts of chlorite.

The uranium content of the clayey fraction is 3.6 ppm, independently of the technique used to concentrate the clay particles, either centrifugation or flocculation. With their uranium content similar to the mean uranium content in the Boom Clay and their abundance (up to 60 wt. %), clay minerals are the main contributors to the total naturally occurring uranium.

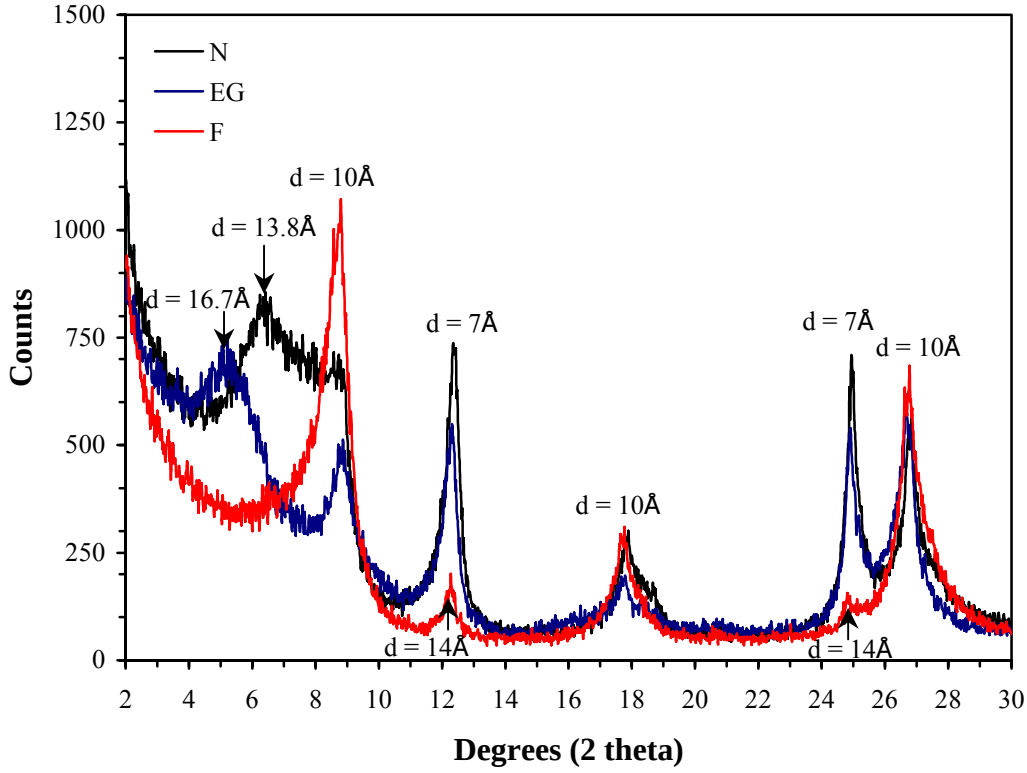

Figure 3.7. XRD patterns of the clayey fraction. N, F and EG are described in the text.

3.5.3.5 Pyrite

The XRD characterisation of the pyrite samples shows that pyrite is the main mineral but quartz is always present. There is no other mineral detected by XRD. As expected from the study of the non-magnetic fractions, pyrite does not show uranium enrichment relative to the Boom Clay content (Table 3.3). The uranium content in all pyrite samples is lower than 1 ppm, with no effect of separation technique (sieving, bromoform, flotation), nor grain-size, nor morphology (framboids or concretions), and nor location (quarry or underground research laboratory). As stated by Yoshida *et al.* (1991), our results confirm that pyrite does not concentrate uranium despite its reducing capacity.

In the frame of its thesis, Cornelis (2003) measured the uranium content in different grain-size fractions of heavy minerals. The heavy minerals were concentrated by sedimentation in bromoform of the residue resulting from the sieving of Boom Clay slurries. The uranium content increased with decreasing grain-size from 0.11 to 7.35 ppm in the 125-500 and 20-32 μm fractions, respectively. In that study, the mineral dissolution was achieved by acidic treatment: 100 mg of the sample were dissolved in a mixture of 1 ml HNO_3, 3 ml HCl and 50 μl HF. To control the effect of the dissolution technique, we have re-analysed our pyrite samples by dissolving the minerals in acid. Doing this, we obtain similar uranium concentration than those measured by alkaline fusion (Table 3.3). Therefore, we ascribed the uranium content measured by Cornelis (2003) to heavy minerals other than pyrite. Indeed, the fraction poor in uranium (125-500 μm) contained only pyrite and quartz while rutile, anatase, carbonates (dolomite, siderite, hydrozincite) were identified by

XRD besides pyrite and quartz in the fractions enriched in uranium (32-63 μm and 20-32 μm).

Table 3.3. Uranium content in the pyrite samples measured after alkaline fusion or acid dissolution.

Samples	Uranium content (ppm)	
	alkaline fusion	acid dissolution
CTP-+1.25 mm	< 1	0.38
CTP-heavy	< 1	0.22
CTP-flotation	1.1	0.47
L-36	< 1	0.82

3.5.3.6 Carbonates

The uranium content is first determined in the bivalve shells. Laenen (1997) mentioned that a notable characteristic of the bivalve shells is its aragonitic composition. Our XRD characterisation confirms that the only mineral forming the shell is aragonite. The uranium content in this biogenic aragonite is lower than 1 ppm.

Secondly, the uranium concentration in septaria was measured for the first time. Although the uranium content varies from one sample to another, the septaria are generally enriched in uranium relative to the mean uranium content in the Boom Clay (Table 3.4). The uranium content strongly depends on the mineralogy of the septaria, and particularly on the presence of siderite. We have measured in the calcitic septaria S30 and S50 uranium content of about 3 and 5 ppm, respectively. The magnesian calcite cement of the S30 concretion has an uranium content below the detection limit. This would indicate that the uranium incorporation in the septaria occurred before the filling of the septarian fractures. The uranium content of the calcitic septaria seems to be related to their stratigraphic location: the S50 concretion situated in the Putte Member contains more uranium than the S30 septaria located in the Terhagen Member (Figure 3.1). This variation might be related to geochemical changes during the deposition of the Putte Member which is enriched in organic matter with respect to the Terhagen Member. Unlike concretions S30 and S50, the septaria S60 is a siderite-rich level that shows uranium contents as high as about 10 ppm in the body of the concretion and 11 ppm in the bioturbations occurring at the surface of the septaria. De Craen *et al.* (2000) reported uranium content up to 83 ppm in the septaria level S60. The uranium association with siderite that was deduced from the statistical analyses by De Craen *et al.* (2000) and that is observed in the magnetic fractions is confirmed by the study of the uranium content in the septaria.

Table 3.4. Uranium content and mineralogical composition of the carbonate concretions (septaria).

Samples	Uranium content ppm	Mineralogy
S30	2.7	calcite, quartz, (clay minerals and feldspar)
S30 cement	< 0.5	magnesian calcite
S50	4.9	calcite, quartz (clay minerals)
S60	9.7	calcite, siderite, quartz, (clay minerals)
S60 bioturbations	11.2	calcite, siderite, quartz, (clay minerals)

3.6 Conclusion

The concentration of natural uranium falls in the range of 10^{-10} to 10^{-8} mol·l^{-1} in Boom Clay pore water and in surrounding aquifers indicating a very homogeneous distribution of mobile uranium. The uranium content in bulk Boom Clay typically varies between 3 and 6 ppm with a mean value of 4 ppm. Most daughter/parent activity ratio of uranium isotopes and daughters measured in bulk Boom Clay samples are equal to unity within the 2σ uncertainties. This means that no important mobility of uranium has been observed in the Boom Clay, at least for the last million years. The variations in uranium content are primary in origin and related to lithological variations.

Statistical analyses and direct measurement show that naturally occurring uranium in the Boom Clay is mainly associated with organic-matter, apatite, authigenic iron-bearing minerals such as ankerite, siderite and glauconite and detrital heavy minerals such as zircon, xenotime, monazite and Ti-oxide. Quartz, feldspar, biogenic aragonite are depleted in uranium relative to the mean uranium content in the Boom Clay. Despite its reducing capacity, pyrite does not concentrate uranium. Although the effect of iron-rich carbonate on the uranium distribution is clearly established, the role of calcite in concentrating uranium is not obvious. It seems that calcite is responsible for the higher uranium content (7 ppm) in the bulk Boom Clay sample from the septaria level S50. On the other hand, calcitic septaria from levels S30 and S50 do not show uranium enrichment. Due to their abundance and their uranium content of about 4 ppm, the clayey fraction (< 2 μm) is the main contributor to the total uranium in the Boom Clay. Uranium is presumably adsorbed to surfaces of clay particles. The sorption capacity of several clay minerals occurring in the Boom Clay towards uranium is discussed in the second part of the Chapter 7.

3.7 References

Cornelis, B. 2003. Pyriet uit de Boomse Klei: scheiding van de verschillende fracties en sorptieproeven met U(6+). Master thesis, Katholieke Hogeschool Kempen.

De Craen, M., Delleuze, D., Volckaert, G., Sneyers, A., Put, M. 2000. The Boom Clay as natural analogue. SCK•CEN report, **R-3444**, Mol, Belgium.

De Craen, M., Wang, L., Van Geet, M., Moors, H. in preparation. Geochemistry of the Boom Clay pore water a the Mol site. SCK•CEN report, **BLG-xxx**, Mol, Belgium.

Dierckx, A., Put, M., De Cannière, P., Wang, L., Maes, N., Aertsens, M., Maes, A., Vancluysen, J., Verdickt, W., Gielen, R., Christiaens, M, Warwick, P., Hall, A., van der Lee, J. 2000. Transport of radionuclides due to complexation with organic matter in clay formations (Trancom-Clay). European Commission Nuclear Science and Technology. Final report **EUR 19135** EN.

Fleischer, R.L. 1988. Alpha-recoil damage: Relation to isotopic disequilibrium and leaching of radionuclides. *Geochimica et Cosmochimica Acta* **52**, 1459-1466.

Gromet, L.P., Dymek, R.F., Haskin, L.A., Korotev, R.L. 1984. The "North American Shale Composite:" its compilation, major and trace element characteristics. *Geochimica et Cosmochimica Acta* **48**, 2469-2482.

Laenen, B. 1997. "The geochemical signature of relative sea-level cycles recognised in the Boom Clay". Ph.D. thesis. K.U.Leuven, Leuven, Belgium.

Laenen, B., Hertogen, J., Vandenberghe, N. 1997. The variation of the trace-element content of fossil biogenic apatite through eustatic sea-level cycles. *Palaeogeography, Palaeoclimatology, Palaeocology* **132**, 325-342.

Marivoet, J., Van Keer, I., Wemaere, I., Hardy, L., Pitsch, H., Beaucaire, C., Michelot, J.-L., Marlin, C., Philippot, A.C., Hassanizadeh, M., van Weert, F. 2000. A PalaeoHYdrogeological study of the MOL site (PHYMOL project). European Commission Nuclear Science and Technology. Final report **EUR 1946** EN.

NIROND 2003-02. 2003. 3D Model of the Boom Clay around the HADES-URF: construction of an AUTOCAD 3D-model of the URF, together with the internal clay layering (ONDRAF/NIRAS ed.).

Vandenberghe, N. 1978. Sedimentology of the Boom Clay (Rupelian) in Belgium. Verhandeling Koninklijke Academie voor Wetenschappen, Letteren en Schone Kunsten van België, Klasse derWetenschappen, jaargang XL, Nr 147.

Yoshida, H., Monsecour, M., Basham, I.R. 1991. Use of microscopic techniques in migration studies on Boom Clay. *Radiochimica Acta* **52/53**, 1333-138.